Anisotropies in scalar-induced gravitational-wave background from inflaton-curvaton mixed scenario with sound speed resonance

Yan-Heng Yu and Sai Wang[*]

Theoretical Physics Division, Institute of High Energy Physics, Chinese Academy of Sciences,
19B Yuquan Road, Shijingshan District, Beijing 100049, China
and School of Physics, University of Chinese Academy of Sciences,
19A Yuquan Road, Shijingshan District, Beijing 100049, China

We propose a new model to generate large anisotropies in the scalar-induced gravitational wave (SIGW) background via sound speed resonance in the inflaton-curvaton mixed scenario. Cosmological curvature perturbations are not only exponentially amplified at a resonant frequency, but also preserve significant non-Gaussianity of local type described by f_{nl}. Besides a significant enhancement of energy-density fraction spectrum, large anisotropies in SIGWs can be generated, because of super-horizon modulations of the energy density due to existence of primordial non-Gaussianity. A reduced angular power spectrum $\tilde{C}_{\ell}$ could reach an amplitude of $[\ell(\ell+1)\tilde{C}_{\ell}]^{1/2} \sim 10^{-2}$, leading to potential measurements via planned gravitational-wave detectors such as DECIGO. The large anisotropies in SIGWs would serve as a powerful probe of the early Universe, shedding new light on the inflationary dynamics, primordial non-Gaussianity, and primordial black hole dark matter.

I. INTRODUCTION

Analogous to the study of cosmic microwave background (CMB) [1,2], the anisotropies in gravitational wave background (GWB) encode crucial information about the primordial Universe, and further, enable us to directly detect the physics during the earlier stages beyond the observational capabilities of CMB, because gravitational waves (GWs) can propagate almost freely since their generation [3,4]. In fact, the dynamics of the early Universe has left imprints on cosmological GWB and hence the anisotropies in GWB serve as a powerful tool to explore this fundamental physics [5]. Though strong evidence for a GWB have been reported [6–9], distinguishing different origins of such a GWB based solely on its energy-density fraction spectrum is challenging, since different physical scenarios might predict the same spectrum. However, the anisotropies in GWB would be useful for differentiating among multiple astrophysical and cosmological sources via examining differences in their angular power spectra [10–52].

As inevitable byproducts of the evolution of linear cosmological curvature perturbations, scalar-induced gravitational waves (SIGWs) [53–59] are considered as a natural cosmological source for the anisotropic GWB [5,12–14, 38–40,60–64], serving as a probe of the inflationary dynamics. SIGWs have attracted lots of interests for the

relationship to many vital topics like primordial non-Gaussianity (PNG) [65–73], which describes the deviation from the Gaussian statistics of primordial curvature perturbations and thus reflects the interactions of quantum fields during inflation. As shown in Refs. [12–15], PNG plays a key role in generating the anisotropies in SIGWs on large scales. It leads to couplings between the large- and small-scale curvature perturbations, resulting in the super-horizon modulation of the energy density of SIGWs, which is manifested as the initial inhomogeneities of SIGWs. Finally, these inhomogeneities lead to the anisotropies in SIGWs. Conversely, the latter can give insights on PNG.

Despite the importance of the anisotropies in GWB, they have not been observed yet in present observations. Only upper limits have been placed on the angular power spectrum by the North American Nanohertz Observatory for Gravitational Waves (NANOGrav) [74], and the LIGO, Virgo, and KAGRA (LVK) [75–77]. Therefore, any cosmological scenario generating significantly anisotropic GWB would attract great attention, since it would open a new window to study the early Universe.

In this work, we will propose a novel model to generate significantly anisotropic SIGWs by sound speed resonance (SSR) [78–81] in the inflaton-curvaton mixed scenario [82–85]. As a nonlinear mechanism, SSR is capable of enhancing primordial curvature perturbations on small scales, although some upper limits on the curvature power spectrum have been established [86–94]. Such an enhancement potentially leads to the production of a large abundance

---

[*]Corresponding author: wangsai@ihep.ac.cn

of primordial black holes (PBHs), which are considered as a competitive candidate of dark matter [95,96]. Meanwhile, the curvaton scenario [97–108] is a class of well-motivated multifield inflationary models with potential to generate a large PNG, which is also considered as a possible non-adiabatic source of anisotropic GWs [109]. Comparing to the curvaton scenario, where the curvature perturbations from inflaton are negligible, the inflaton-curvaton mixed scenario incorporates the curvature perturbations from both the inflaton and the curvaton. The inflaton-curvaton mixed scenario with SSR was firstly studied in Ref. [80], in which the curvaton acts as a spectator scalar field and is assumed to undergo SSR to create enhanced entropy perturbations during inflation. When the curvaton decays into the radiation after inflation, these perturbations convert into curvature perturbations with a peaked feature in primordial curvature power spectrum and a large PNG, which are both crucial for generating significantly anisotropies in SIGWs. The proposed model could be realized by combining curvaton scenario with D-brane dynamics in string theory [110,111], k-inflation [112,113], another coupled field with heavy modes integrated out in the effective field theory [114–116], and so on.

We will also show that the anisotropies in SIGWs, with a reduced angular power spectrum $\ell(\ell+1)\tilde{C}_\ell \sim 10^{-4}$, could be larger by five orders of magnitude than those in CMB. This spectrum is potentially measured in future by multiband GW detectors, such as LVK [117–119], Einstein Telescope (ET) [120], Laser Interferometer Space Antenna (LISA) [121,122], Taiji [123], Square Kilometer Array (SKA) [124], and Deci-hertz Interferometer Gravitational wave Observatory (DECIGO) [125,126]. Once being observed, it would serve as a powerful probe of both PNG and PBHs, and give implications for the inflationary dynamics.

A. Inflaton-curvaton mixed scenario with SSR

We briefly review the inflaton-curvaton mixed scenario, following the conventions of Refs. [82–85]. Besides the inflaton ϕ, there is a spectator field, i.e., the curvaton χ, with its mass satisfying $m_\chi \ll H$, where H is the Hubble parameter during inflation. The fields ϕ and χ are weakly coupled, and can be decomposed into their background components ($\bar{\phi}$ and $\bar{\chi}$) and fluctuations ($\delta\phi$ and $\delta\chi$), with the assumption that these fluctuations are Gaussian. While $\delta\phi$ generates the curvature perturbations ζ_ϕ, $\delta\chi$ conveys the entropy perturbations $\mathcal{S}_\chi$, which subsequently transform into the curvature perturbations ζ_χ when χ decays into radiation after the end of inflation but before the start of primordial nucleosynthesis, as constrained by CMB observations [2]. Therefore, the total curvature perturbations ζ_{tot} are comprised of contributions from both ζ_ϕ and ζ_χ. Though χ subdominates the energy density of the inflationary Universe, ζ_χ can be comparable to ζ_ϕ or even dominant.

In this model, $\delta\chi$ undergoes SSR during inflation [80]. On spatially flat slices, the evolution of $\delta\chi_k$ obeys the Mukhanov-Sasaki (MS) equation, i.e., [127,128]

$$v_k''(\eta) + \left(c_s^2 k^2 - \frac{z''}{z}\right)v_k(\eta) = 0, \qquad (1)$$

where we define $v_k = a\delta\chi_k/c_s$ and $z = a\bar{\chi}'/(c_s\mathcal{H})$, a prime denotes a derivative with respect to the conformal time η, c_s is the sound speed, a is a scale factor of the Universe, and $\mathcal{H}$ is a conformal Hubble parameter. We suppose that c_s oscillates with η, namely [78],

$$c_s^2(\eta) = 1 - 2\xi[1 - \cos(2k_0\eta)], \qquad (2)$$

where ξ and k_0 stand for the oscillating amplitude and frequency, respectively. The oscillation begins at η_i, which is deep in the horizon, i.e., $-k_0\eta_i \gg 1$, and ends at the horizon exit $-k_0\eta_e \simeq 1$. In the limit of slow-roll approximation and due to the temporal oscillation of c_s, the MS equation can be recast into the Mattieu equation, which is a characteristic of SSR, i.e., [80]

$$\frac{d^2 v_k}{dx^2} + (A_k - 2B_k \cos 2x)v_k = 0. \qquad (3)$$

Here, we introduce $x = -k_0\eta$, $A_k = (k^2/k_0^2)(1 - 2\xi)$, and $B_k = (2 - k^2/k_0^2)\xi$, with an approximation of $\xi \ll 1$. One of important features of the Mattieu equation is that v_k (and equivalently $\delta\chi_k$) is exponentially amplified at a characteristic scale $k_S \sim (1 + \xi)k_0$ with resonant width $\sim\xi k_0$, indicating an amplification factor $|v_{k_S}/v_{k\neq k_S}| \sim e^{-\xi k_S\eta/2}$ [78,80]. The amplified $\delta\chi$ finally leads to an enhancement of ζ_{tot} at around k_S, as showed in the following.

B. Primordial curvature perturbations

We investigate ζ_j ($j = \phi, \chi, \text{tot}$) using δN formalism [103,129–131]. In this formalism, the superhorizon ζ_j on uniform-ρ_{tot} slices can be expressed as [103,132]

$$\zeta_j(t, \mathbf{x}) = \delta N(t, \mathbf{x}) + \frac{1}{3}\int_{\bar{\rho}_j(t)}^{\rho_j(t,\mathbf{x})} \frac{d\rho_j'}{(1 + w_j)\rho_j'}. \qquad (4)$$

Here, ρ_j (and $\bar{\rho}_j$) is the local (and background) energy density, w_j is the equation-of-state parameter, and δN is the local perturbation expansion from the initial spatially flat slice to the final uniform-ρ_{tot} slice. Specially, Eq. (4) naturally gives $\zeta_{\text{tot}} = \delta N$ on a uniform-ρ_{tot} slice.

Firstly, we consider the generation of entropy perturbations $\mathcal{S}_\chi = 3(\zeta_\chi - \zeta_\phi)$ arising from $\delta\chi$ [100]. At the end of inflation, ϕ decays into radiation, which inherits ρ_ϕ and ζ_ϕ from ϕ. Since that time, both the radiation and χ are relativistic until H decreases to m_χ. Once $H \sim m_\chi$, χ begins to oscillate around the bottom of its potential and behaves

as pressureless matter with $\rho_\chi = m_\chi^2 \chi_{\rm osc}^2$ [84], where $\chi_{\rm osc}$ represents the root-mean-square value of the oscillating curvaton. The uniform-$\rho_{\rm tot}$ slice at the beginning of the oscillation is characterized as $\zeta_\phi = \delta N$, since ρ_χ is still subdominant [84]. Equation (4) gives $\rho_\chi = \bar{\rho}_\chi e^{3(\zeta_\chi - \zeta_\phi)} = \bar{\rho}_\chi e^{S_\chi}$ on this slice, leading to a relation between S_χ and $\delta\chi_{\rm osc}$ through ρ_χ, i.e.,

$$m_\chi^2(\bar{\chi}_{\rm osc} + \delta\chi_{\rm osc})^2 = m_\chi^2 \bar{\chi}_{\rm osc}^2 e^{S_\chi}. \qquad (5)$$

In this work, we assume that χ has a quadratic potential, which indicates that $\delta\chi_{\rm osc}/\bar{\chi}_{\rm osc} = \delta\chi_*/\bar{\chi}_*$ is a constant [98,100,133], with $_*$ denoting the field value at horizon exit. With this assumption, we further connect S_χ to $\delta\chi_*$ by expanding Eq. (5) up to the second order, i.e.,

$$S_\chi = 2\frac{\delta\chi_*}{\bar{\chi}_*} - \left(\frac{\delta\chi_*}{\bar{\chi}_*}\right)^2 = S_{\chi,g} - \frac{1}{4}S_{\chi,g}^2, \qquad (6)$$

where we introduce $S_{\chi,g} = 2\delta\chi_*/\bar{\chi}_*$ to represent a Gaussian component of S_χ.

Secondly, S_χ convert into adiabatic perturbations and contribute to $\zeta_{\rm tot}$. During the oscillation phase, $\rho_\chi/\rho_{\rm tot}$ continues to increase while S_χ remain constant. When H drops to the decay rate of χ, we assume that χ suddenly decays into radiation on a uniform-$\rho_{\rm tot}$ slice. This slice is characterized by $\delta N = \zeta_{\rm tot}$, where $\zeta_{\rm tot}$ is valued at the time right after the decay. Therefore, Eq. (4) implies the following relation [103]:

$$\Omega_{\chi,{\rm d}} e^{3(\zeta_\chi - \zeta_{\rm tot})} + (1 - \Omega_{\chi,{\rm d}}) e^{4(\zeta_\phi - \zeta_{\rm tot})} = 1, \qquad (7)$$

with $\Omega_{\chi,{\rm d}}$ being the energy-density fraction of χ at the time right before the decay. Equation (7) completely determines the relation between $\zeta_{\rm tot}$ and ζ_χ. We further expand Eq. (7) to the second order and express $\zeta_{\rm tot}$ in terms of S_χ, namely,

$$\begin{aligned}
\zeta_{\rm tot} &= \zeta_\phi + \frac{r}{3}S_\chi + \frac{r(1-r)(3+r)}{18}S_\chi^2 \\
&= \zeta_\phi + \frac{r}{3}S_{\chi,g} + \frac{r}{18}\left(\frac{3}{2} - 2r - r^2\right)S_{\chi,g}^2,
\end{aligned} \qquad (8)$$

where we define $r = 3\Omega_{\chi,{\rm d}}/(4 - \Omega_{\chi,{\rm d}})$ with $0 < r < 1$. Through Eqs. (6) and (8), the nonlinear evolution of $\delta\chi$ during inflation can be reflected on $\zeta_{\rm tot}$.

Here, we investigate a dimensionless primordial power spectrum $\Delta_{\zeta_g}^2$ for the Gaussian curvature perturbations ζ_g. In Eq. (8), we assume that ζ_ϕ is Gaussian, so the Gaussian component of $\zeta_{\rm tot}$ is $\zeta_g = \zeta_\phi + (r/3)S_{\chi,g}$. For convenience, we introduce $\lambda(k)$ to parametrize $\Delta_{\zeta_g}^2$ as $\Delta_{\zeta_g}^2 = \Delta_{\zeta_\phi}^2 + \Delta_{\zeta_\chi}^2 = [1 + \lambda(k)]\Delta_{\zeta_\phi}^2$, where $\Delta_{\zeta_\phi}^2$ is a scale-invariant spectrum and $\lambda(k) \propto k|(v_k)_*|^2$ [80] is scale dependent. On large scales related to $k_{\rm L}$, λ is taken as a scale-invariant value, as

denoted by $\lambda_{\rm L}$. On small scales at around $k_{\rm S}$, λ is exponentially amplified and given by $\lambda_{\rm S} \sim \lambda_{\rm L} e^{-\xi k_{\rm S}\eta_i} \sim \lambda_{\rm L} e^{\xi e^{\Delta N}}$ [80], where ΔN is the e-folding number during SSR. Therefore, we separate ζ_g as $\zeta_g = \zeta_{g{\rm L}} + \zeta_{g{\rm S}}$ [134], where $\zeta_{g{\rm L}}$ is the large-scale component at $k_{\rm L}$ contributed from both ζ_ϕ and $S_{\chi,g}$ of nonresonant modes, while $\zeta_{g{\rm S}}$ is the small-scale component at $k_{\rm S}$ arising from $S_{\chi,g}$ of resonant modes. Phenomenologically, we model $\Delta_{\zeta_g}^2$ as a scale-invariant background $\Delta_{\zeta_{g{\rm L}}}^2$ plus a resonant peak $\Delta_{\zeta_{g{\rm S}}}^2$ centered at $k_{\rm S}$, i.e.,

$$\Delta_{\zeta_g}^2(k) = \Delta_{\zeta_{g{\rm L}}}^2 + \Delta_{\zeta_{g{\rm S}}}^2 = \mathcal{A}_{\rm L} + \frac{\mathcal{A}_{\rm S}}{\sqrt{2\pi}\sigma} e^{-\frac{1}{2\sigma^2}\ln^2(k/k_{\rm S})}, \qquad (9)$$

where the large-scale spectral amplitude $\mathcal{A}_{\rm L}$ is extrapolated from observations of CMB, i.e., $\mathcal{A}_{\rm L} \simeq 2.1 \times 10^{-9}$ at a pivot scale $k_{\rm p} = 0.05$ Mpc^{-1} [1]. On small scales, the spectral width σ depends on the resonant width $\sim\xi k_0$. For example, we get $\sigma \sim 10^{-2}$ when considering $\xi \sim 0.1$. The small-scale spectral amplitude $\mathcal{A}_{\rm S}$ is determined by $\mathcal{A}_{\rm S}/\mathcal{A}_{\rm L} \sim (\xi/2)e^{\xi e^{\Delta N}}$. It describes the enhancement of ζ_g and could be closely related to the formation of PBHs [78–81]. For example, $\Delta N \sim 5.4$ (or 10.2) is enough for $\xi \sim 10^{-1}$ (or 10^{-3}) to induce $\mathcal{A}_{\rm S} \sim \mathcal{O}(1)$, implying an efficient mechanism to produce abundant PBHs.

II. PRIMORDIAL NON-GAUSSIANITY

In the proposed model, the local-type PNG, as denoted by $f_{\rm nl}$, is not only large, but also scale dependent. The non-Gaussian curvature perturbations $\zeta_{\rm tot}$ can be parametrized by the Gaussian one ζ_g, i.e., [135],

$$\zeta_{\rm tot,\mathbf{k}} = \zeta_{g,\mathbf{k}} + \frac{3}{5}\int \frac{d^3\mathbf{p}}{(2\pi)^{3/2}} f_{\rm nl}(k, p, |\mathbf{k} - \mathbf{p}|)\zeta_{g,\mathbf{k}-\mathbf{p}}\zeta_{g,\mathbf{p}}. \qquad (10)$$

Based on Eqs. (8) and (10), $f_{\rm nl}$ can be read as [84,85]

$$f_{\rm nl}(k_1, k_2, k_3) = \left(\frac{5}{4r} - \frac{5}{3} - \frac{5r}{6}\right)\alpha(k_1, k_2, k_3), \qquad (11)$$

where $\alpha = \Sigma'(r/3)^4 P_{S_{\chi,g}}(k_1)P_{S_{\chi,g}}(k_2)/\Sigma' P_{\zeta_g}(k_1)P_{\zeta_g}(k_2)$ with $P(k) = (2\pi^2/k^3)\Delta^2(k)$ being a dimensional power spectrum. Here, we introduce a symbol Σ' to represent $\Sigma' P(k_1)P(k_2) = P(k_1)P(k_2) + P(k_2)P(k_3) + P(k_3)P(k_1)$.

The PNG $f_{\rm nl}$ in Eq. (11) has two obvious features. One concerns that a large $f_{\rm nl}$ can be generated if r is small, which implies that the nonlinear fluctuation should be more violent for a more subdominant χ to generate a certain amount of curvature perturbations. The other one is that $f_{\rm nl}$ is scale dependent. Considering the scale dependence of $\lambda(k)$ and $P(k_{\rm L}) \gg P(k_{\rm S})$, we can approximate the scale-dependent $\alpha(k_1, k_2, k_3)$ in Eq. (11) in the squeezed limit $k_1 \approx k_2 \gg k_3$ as follows:

$$\alpha \simeq \begin{cases} (1 + \lambda_L^{-1})^{-2}, k_1, k_2, k_3 \text{ at large scales,} \\ (1 + \lambda_S^{-1})^{-2}, k_1, k_2, k_3 \text{ at small scales,} \\ [(1 + \lambda_S^{-1})(1 + \lambda_L^{-1})]^{-1}, \end{cases}$$

$$k_1, k_2 \text{ at small scales, } k_3 \text{ at large scales.} \qquad (12)$$

For simplicity, we denote f_{nl} in the three cases in Eq. (12) as $f_{nl,L}$, $f_{nl,S}$, and $f_{nl,LS}$, respectively. $f_{nl,L}$ is constrained by the observations of CMB as $f_{nl,L} = -0.9 \pm 5.1$ at 68% confidence level [136], $f_{nl,S}$ with $\lambda_S \gg 1$ reduces to the standard result of the curvaton scenario [102–105], while $f_{nl,LS}$ describes the strength of nonlinear couplings between the large- and small-scale perturbations. As will be demonstrated, $f_{nl,S}$ and $f_{nl,LS}$ play key roles in the energy-density fraction spectrum and the angular power spectrum of SIGWs, respectively. They are constrained by measurements of $f_{nl,L}$ via $f_{nl,LS}^2 \simeq f_{nl,L} f_{nl,S}$.

III. ENERGY-DENSITY FRACTION SPECTRUM OF SIGWs

The energy density of SIGWs could be decomposed as $\rho_{gw}(\eta, \mathbf{x}) = \bar{\rho}_{gw}(\eta) + \delta\rho_{gw}(\eta, \mathbf{x})$, where $\mathbf{x}$ is the coarse-grained location depending on the finite angular resolution of GW detectors, $\bar{\rho}_{gw}$ is the homogeneous and isotropic background, and $\delta\rho_{gw}$ stands for the inhomogeneities on this background. Corresponding to $\bar{\rho}_{gw}$ and $\delta\rho_{gw}$, we define the energy-density fraction spectrum $\bar{\Omega}_{gw}$ and the density contrast δ_{gw} of SIGWs, which are given by [137]

$$\bar{\rho}_{gw}(\eta) = \rho_c(\eta) \int d\ln q \, \bar{\Omega}_{gw}(\eta, q), \qquad (13a)$$

$$\delta\rho_{gw}(\eta, \mathbf{x}) = \rho_c(\eta) \int d\ln q \, d^2\hat{\mathbf{q}} \frac{1}{4\pi} \bar{\Omega}_{gw}(\eta, q) \delta_{gw}(\eta, \mathbf{x}, \mathbf{q}). \qquad (13b)$$

Here, we introduce $q = |\mathbf{q}|$ and $\hat{\mathbf{q}} = \mathbf{q}/q$ with $\mathbf{q}$ being the wave vector of SIGWs, and ρ_c is the critical energy density of the Universe at η. We focus solely on Eq. (13) in this section while leave Eq. (13b) to a study of the anisotropies in SIGWs in the next section.

At the production time η_{in} of SIGWs, the energy-density fraction spectrum is given by $\bar{\Omega}_{gw}(\eta_{in}, q) \sim \langle \zeta_{tot}^4 \rangle$ [53,54], where $\langle \dots \rangle$ stands for the spatial average. When evaluating $\bar{\Omega}_{gw}$, we can simply treat ζ_{tot} as the small-scale curvature perturbations $\zeta_S = \zeta_{gS} + (3/5)f_{nl,S}\zeta_{gS}^2$, since contributions from the large-scale ones is negligible due to $\mathcal{A}_L \ll \mathcal{A}_S$. Therefore, for small scales of observational interest, we obtain $\bar{\Omega}_{gw} \sim \langle \zeta_S^4 \rangle$. Its complete analysis has been presented in Refs. [13,14,138–140]. Other related works can be found in Refs. [141–151].
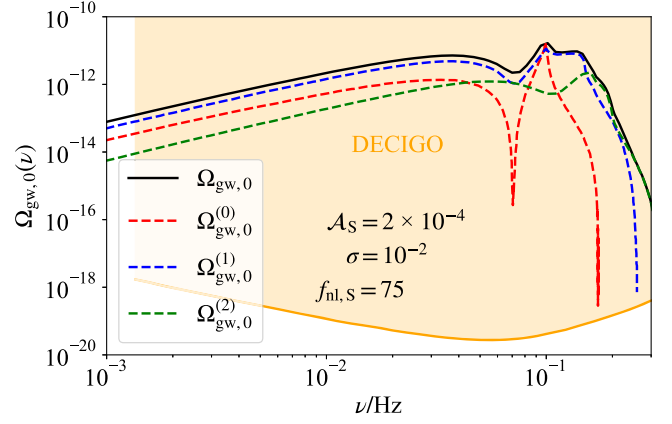

FIG. 1. Energy-density fraction spectrum $\bar{\Omega}_{gw,0}(\nu)$ (black solid curve) and its components $\bar{\Omega}_{gw,0}^{(0)}$ (red dashed curve), $\bar{\Omega}_{gw,0}^{(1)}$ (blue dashed curve), and $\bar{\Omega}_{gw,0}^{(2)}$ (green dashed curve) at the frequency $\nu_{peak} = 0.1$ Hz. For comparison, the sensitivity of DECIGO is displayed as the orange shaded region.

The present-day energy-density fraction spectrum of SIGWs is given by [152]

$$\bar{\Omega}_{gw,0}(\nu) \simeq \Omega_{rad,0} \bar{\Omega}_{gw}(\eta_{in}, q)|_{q=2\pi\nu}, \qquad (14)$$

where the present-day physical energy-density fraction of radiation is $h^2\Omega_{rad,0} = 4.2 \times 10^{-5}$ with the dimensionless Hubble constant $h = 0.674$ [1]. For simplicity, we denote the $\mathcal{O}(f_{nl,S}^{2m})$ component of $\bar{\Omega}_{gw,0}$ as $\bar{\Omega}_{gw,0}^{(m)}$ ($m = 0, 1, 2$). In Fig. 1, we depict $\bar{\Omega}_{gw,0}$ and $\bar{\Omega}_{gw,0}^{(m)}$ with variable $\nu = q/(2\pi)$, and compare them with the sensitivity curve of DECIGO [153]. It is shown that $\bar{\Omega}_{gw,0}$ is enhanced at around $\nu_{peak} = (2/\sqrt{3})(k_S/2\pi)$, and a large $f_{nl,S}$ enlarges the spectral amplitude and obviously changes the spectral index.

A. Angular power spectrum of SIGWs

Following Refs. [12–14], we show that in Eq. (13b), the large-scale $\delta\rho_{gw}$ leads to the anisotropies in SIGWs. Here, we disregard the small-scale inhomogeneities, because the horizon at $(\eta_{in}, \mathbf{x}_{in})$ is extremely small for the present-day observer at $(\eta_0, \mathbf{x}_0)$, and the observed energy density along a line-of-sight is an average over a quantity of such horizons [12–15]. The observed large-scale $\delta_{gw}(\eta_0, \mathbf{x}_0, \mathbf{q})$ in Eq. (13b) is contributed by both the initial density contrast and the Sachs-Wolfe effect [154], i.e.,

$$\delta_{gw}(\eta_0, \mathbf{x}_0, \mathbf{q}) = \delta_{gw}(\eta_{in}, \mathbf{x}_{in}, \mathbf{q}) + [4 - n_{gw,0}(\nu)]\Phi(\eta_{in}, \mathbf{x}_{in}), \qquad (15)$$

where we define $n_{gw,0}(\nu) = \partial \ln \bar{\Omega}_{gw,0}(\nu)/\partial \ln \nu$, and the Bardeen potential follows $\Phi(\eta_{in}, \mathbf{x}_{in}) \propto \zeta_{gL}$. Compared

with the Sachs-Wolfe effect, the integrated Sachs-Wolfe effect is negligible [12].

In Eq. (15), we focus on the term $\delta_{gw}(\eta_{in}, \mathbf{x}_{in}, \mathbf{q})$, which arises from $f_{nl,LS}$, indicating the couplings between ζ_{gL} and ζ_{gS}. Such couplings can spatially modulate the energy density of SIGWs, which were produced by ζ_S, on super-horizon scales. To demonstrate this picture, we expand $\bar{\Omega}_{gw} \sim \langle \zeta_{tot}^4 \rangle$ according to the order of ζ_{gL}, i.e.,

$$\langle \zeta_{tot}^4 \rangle \sim \langle \zeta_S^4 \rangle + \mathcal{O}(\zeta_{gL}) f_{nl,LS} \langle \zeta_{gS} \zeta_S^3 \rangle + \mathcal{O}(\zeta_{gL}^2). \quad (16)$$

The large-scale $\delta_{gw}(\eta_{in}, \mathbf{x}_{in}, \mathbf{q})$ can be obtained from the $\mathcal{O}(\zeta_{gL})$ component of $\langle \zeta_{tot}^4 \rangle$, leading to $\delta_{gw}(\eta_{in}, \mathbf{x}_{in}, \mathbf{q}) \sim \mathcal{O}(\zeta_{gL}) f_{nl,LS} \langle \zeta_{gS} \zeta_S^3 \rangle$ at the first order [12–15]. This formula implies that a large amplitude of $f_{nl,LS}$ leads to significant initial inhomogeneities in SIGWs. Moreover, higher-order components of $\langle \zeta_{tot}^4 \rangle$ are negligible due to $\mathcal{A}_L \ll \mathcal{A}_S$.

The observed anisotropies in SIGWs, as characterized by a reduced angular power spectrum $\tilde{C}_\ell$, arise from the large-scale $\delta_{gw}(\eta_0, \mathbf{x}_0, \mathbf{q})$. With the assumption of the cosmological principle, we define $\tilde{C}_\ell$ as follows:

$$\langle \delta_{gw,0,\ell m}(q) \delta_{gw,0,\ell'm'}^*(q) \rangle|_{q=2\pi\nu} = \delta_{\ell\ell'} \delta_{mm'} \tilde{C}_\ell(\nu), \quad (17)$$

where $\delta_{gw,0,\ell m}(q)$ represents the coefficients of the spherical harmonic expansion of $\delta_{gw}(\eta_0, \mathbf{x}_0, \mathbf{q})$, i.e.,

$$\delta_{gw}(\eta_0, \mathbf{x}_0, \mathbf{q}) = \sum_{\ell m} \delta_{gw,0,\ell m}(q) Y_{\ell m}(\hat{\mathbf{q}}). \quad (18)$$

Though two ζ_{gS} with a large angular separation are uncorrelated, ζ_{gL} serves as a "bridge" to correlate them. Hence, we get $\tilde{C}_\ell \sim \langle \delta_{gw}^2(\eta_0, \mathbf{x}_0, \mathbf{q}) \rangle \propto \langle \zeta_{gL}^2 \rangle \sim \Delta_{\zeta_{gL}}^2$. Following a diagrammatic approach, Ref. [13] presented comprehensive calculations of $\tilde{C}_\ell$. The result is given as

$$\tilde{C}_\ell(\nu) = \frac{18\pi \mathcal{A}_L}{25\ell(\ell+1)} \left[f_{nl,LS} \frac{\Omega_{ng,0}}{\bar{\Omega}_{gw,0}} + (4 - n_{gw,0}) \right]^2, \quad (19)$$

where we introduce $\Omega_{ng,0} = 2^3 \bar{\Omega}_{gw,0}^{(0)} + 2^2 \bar{\Omega}_{gw,0}^{(1)}$ as a short-hand notation. The first and second terms in the square brackets inherit from Eq. (15) the initial inhomogeneities and the Sachs-Wolfe effect, respectively.

We demonstrate that large anisotropies in SIGWs can be generated in our model. We consider that the energy density fraction of the curvaton is small at the time of its decay and the curvature perturbations from curvaton are comparable to those of inflation at $\sim k_L$ while dominant at $\sim k_S$. Specifically, we quantify these as $(r = 0.017, \lambda_L = 0.5, \lambda_S \gg 1)$, resulting in PNG ($f_{nl,S} = 75, f_{nl,LS} = 25, f_{nl,L} = 8.3$) through Eqs. (11) and (12). We further quantify the SSR parameters as $\{\xi \simeq 0.12, \Delta N \simeq 4.8\}$, leading to $\{\mathcal{A}_S = 2 \times 10^{-4}, \sigma = 10^{-2}\}$ in Eq. (9), which are within
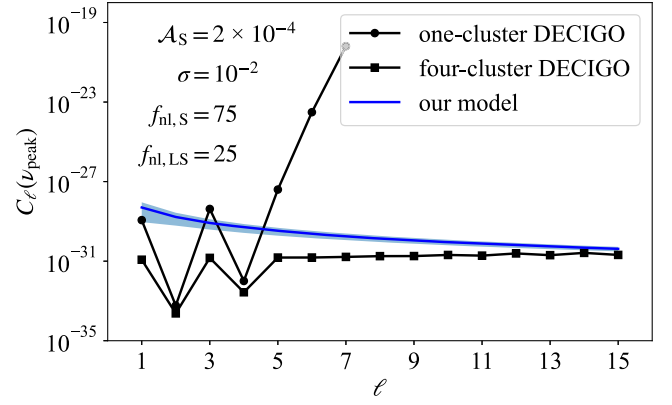

FIG. 2. Angular power spectrum anticipated by our model (blue curve) versus the sensitivity curves of DECIGO (black curves) at the frequency $\nu_{peak} = 0.1$ Hz. The black circles and squares represent the noise angular power spectra at each multipole ℓ for one-cluster and four-cluster DECIGO, respectively [155]. Shaded blue region signifies an inevitable uncertainty at 68% confidence level due to the cosmic variance, i.e., $\Delta C_\ell / C_\ell = \sqrt{2/(2\ell+1)}$.

the constraints from various observations [78]. Therefore, we anticipate the reduced angular power spectrum at around ν_{peak} to be

$$\sqrt{\ell(\ell+1) \tilde{C}_\ell(\nu_{peak})} \sim 10^{-2}. \quad (20)$$

Regarding observations, we define an angular power spectrum as $C_\ell(\nu) = [\bar{\Omega}_{gw,0}(\nu)/4\pi]^2 \tilde{C}_\ell(\nu)$. It could reach $\ell(\ell+1) C_\ell \sim 10^{-28}$, which is potentially observable for future GW detectors like DECIGO [125,126]. In Fig. 2, we depict the anticipated C_ℓ at $\nu_{peak} = 0.1$ Hz and compare it with the sensitivity curve of DECIGO in the same frequency band. Moreover, we show an inevitable uncertainty (68% confidence level) due to the cosmic variance in a blue shaded region.

While the C_ℓ above may not be sufficiently large for detection by LISA, adjusting the parameters in our model could potentially yield an observable angular power spectrum, say, $C_\ell \sim 10^{-23}$ at around $\nu_{peak} = 1$ mHz, for two LISA-like clusters [155]. However, the corresponding $\tilde{C}_\ell$ may not be so large. The maximum achievable anisotropies would only be around $[\ell(\ell+1) \tilde{C}_\ell]^{1/2} \sim 10^{-3}$, where the parameters could be set as $\{\mathcal{A}_S = 8 \times 10^{-3}, \sigma = 10^{-2}, f_{nl,S} = 15, f_{nl,LS} = 12, f_{nl,L} = 10\}$.

IV. CONCLUSIONS AND DISCUSSION

In this work, we showed that the large anisotropies in SIGWs are generated when the curvaton undergoes SSR in the inflaton-curvaton mixed scenario. Introduced by SSR, the exponentially amplified curvature perturbations could induce the enhanced energy-density fraction spectrum of SIGWs around the resonant frequency. The large PNG in

this model leads to a large-scale modulation of the energy density of SIGWs, resulting in the large anisotropies, i.e., $[\ell(\ell+1)\tilde{C}_\ell]^{1/2} \sim 10^{-2}$. These anisotropies have potential to be detected by future GW detectors like DECIGO.

We may use both the energy-density fraction spectrum $\bar{\Omega}_{\mathrm{gw},0}$ and the angular power spectrum C_ℓ of SIGWs as complementary probes to study the dynamics of the early Universe. The peaked feature in both spectra might serve as a characteristic GW signature of this model. The peak width and frequency encode the amplitude ξ and mode k_0 of the oscillation of c_s^2, respectively, while the peak amplitude says the duration of SSR, characterized by ΔN. Additionally, the imprints of $f_{\mathrm{nl,S}}$ and $f_{\mathrm{nl,LS}}$ in $\bar{\Omega}_{\mathrm{gw},0}$ and C_ℓ enable us to explore the parameter space of $\{r, \lambda_{\mathrm{L}}, \lambda_{\mathrm{S}}\}$, which carries vital information about the contributions from curvaton to energy density and curvature perturbations. The measurement of all these parameters is helpful in testing various inflationary models.

Different from the existing studies in Ref. [13], which assumed the scale independence of f_{nl}, our present work considered the scale dependence of f_{nl}. The anisotropies in SIGWs offer a remarkable method to measure $f_{\mathrm{nl,LS}}$, which reveals underlying physics of the nonlinear couplings between long- and short-wavelength modes. These anisotropies may initiate a lot of interests in the model-building studies related with the scale-dependent PNG. When higher-order PNG such as g_{nl} is incorporated [14], our result in Eq. (20) would not change too much due to $|g_{\mathrm{nl}}| \ll f_{\mathrm{nl}}^2$ when $r \ll 1$ in this model [85,103].

The proposed model can lead to efficient production of PBHs, shedding new insights on the nature of cold dark matter. Considering the large positive $f_{\mathrm{nl,S}}$, we roughly estimate the abundance of PBHs as [156,157]

$$
\begin{aligned}
f_{\mathrm{PBH}} \simeq 2.5 \times 10^8 \left(\frac{g_{*,\mathrm{f}}}{10.75}\right)^{-\frac{1}{4}} \left(\frac{\nu}{5.0 \text{ nHz}}\right) \\
\times \frac{1}{2} \mathrm{erfc}\left(\frac{\sqrt{1 + 4\zeta_c(3f_{\mathrm{nl,S}}/5)} - 1}{2(3f_{\mathrm{nl,S}}/5) \times \sqrt{2\mathcal{A}_{\mathrm{S}}}}\right),
\end{aligned} \quad (21)
$$

where $g_{*,\mathrm{f}}$ stands for the number of relativistic degrees of freedom at the formation time of PBHs, ζ_c is the critical curvature perturbation for gravitational collapse, and $\mathrm{erfc}(x)$ denotes the complementary error function with variable x. If considering $g_{*,\mathrm{f}} \sim 100$ [158] and $\zeta_c = 0.7$ [159], we can obtain $f_{\mathrm{PBH}} \sim 1$ at $\nu \sim 0.1$ Hz with the parameters adopted in this work. All of cold dark matter could be accounted for by these abundant PBHs in the asteroid mass range, which has not been explored by the present observations [64]. However, we should note that the above estimation is sensitively model-dependent. For instance, altering the value of ζ_c, considering the f_{nl}-dependence of ζ_c, or employing other methods based on the critical density contrast δ_c could potentially impact the resulting f_{PBH}.

Our model could also be extended into more general cases. For example, a different expression for c_s^2 oscillation from Eq. (2) will not change our framework to obtain an enhanced $\mathcal{A}_{\mathrm{S}}$. Additionally, alternative resonant mechanisms, such as an oscillating inflaton potential [160–166], could also be considered. Furthermore, if considering a nonquadratic potential for χ, the evolution of χ between the horizon exit and oscillating phase would necessitate numerical investigation. While this could lead to some modifications in f_{nl}, the picture of generating large f_{nl} with a small r will remain unchanged [85,103].

[1] N. Aghanim *et al.* (Planck Collaboration), Astron. Astrophys. **641**, A6 (2020); **652**, C4(E) (2021).

[2] Y. Akrami *et al.* (Planck Collaboration), Astron. Astrophys. **641**, A10 (2020).

[3] N. Bartolo, A. Hoseinpour, G. Orlando, S. Matarrese, and M. Zarei, Phys. Rev. D **98**, 023518 (2018).

[4] R. Flauger and S. Weinberg, Phys. Rev. D **99**, 123030 (2019).

[5] N. Bartolo *et al.* (LISA Cosmology Working Group), J. Cosmol. Astropart. Phys. 11 (2022) 009.

[6] G. Agazie *et al.* (NANOGrav Collaboration), Astrophys. J. Lett. **951**, L8 (2023).

[7] J. Antoniadis *et al.* (EPTA Collaboration), arXiv:2306 .16214.

[8] D. J. Reardon *et al.*, Astrophys. J. Lett. **951**, L6 (2023).

[9] H. Xu *et al.*, Res. Astron. Astrophys. **23**, 075024 (2023).

[10] N. Bartolo, D. Bertacca, S. Matarrese, M. Peloso, A. Ricciardone, A. Riotto, and G. Tasinato, Phys. Rev. D **100**, 121501 (2019).

[11] N. Bartolo, D. Bertacca, S. Matarrese, M. Peloso, A. Ricciardone, A. Riotto, and G. Tasinato, Phys. Rev. D **102,** 023527 (2020).

[12] N. Bartolo, D. Bertacca, V. De Luca, G. Franciolini, S. Matarrese, M. Peloso, A. Ricciardone, A. Riotto, and G. Tasinato, J. Cosmol. Astropart. Phys. 02 (2020) 028.

[13] J.-P. Li, S. Wang, Z.-C. Zhao, and K. Kohri, arXiv:2305 .19950.

[14] J.-P. Li, S. Wang, Z.-C. Zhao, and K. Kohri, arXiv:2309 .07792.

[15] S. Wang, Z.-C. Zhao, J.-P. Li, and Q.-H. Zhu, arXiv: 2307.00572.

[16] E. Dimastrogiovanni, M. Fasiello, A. Malhotra, and G. Tasinato, J. Cosmol. Astropart. Phys. 01 (2023) 018.

[17] C. R. Contaldi, Phys. Lett. B **771,** 9 (2017).

[18] A. C. Jenkins, R. O'Shaughnessy, M. Sakellariadou, and D. Wysocki, Phys. Rev. Lett. **122,** 111101 (2019).

[19] A. C. Jenkins, M. Sakellariadou, T. Regimbau, and E. Slezak, Phys. Rev. D **98,** 063501 (2018).

[20] A. C. Jenkins and M. Sakellariadou, Phys. Rev. D **100,** 063508 (2019).

[21] A. C. Jenkins, J. D. Romano, and M. Sakellariadou, Phys. Rev. D **100,** 083501 (2019).

[22] D. Bertacca, A. Ricciardone, N. Bellomo, A. C. Jenkins, S. Matarrese, A. Raccanelli, T. Regimbau, and M. Sakellariadou, Phys. Rev. D **101,** 103513 (2020).

[23] G. Cusin, C. Pitrou, and J.-P. Uzan, Phys. Rev. D **96,** 103019 (2017).

[24] G. Cusin, C. Pitrou, and J.-P. Uzan, Phys. Rev. D **97,** 123527 (2018).

[25] G. Cusin, I. Dvorkin, C. Pitrou, and J.-P. Uzan, Phys. Rev. Lett. **120,** 231101 (2018).

[26] G. Cusin, I. Dvorkin, C. Pitrou, and J.-P. Uzan, Mon. Not. R. Astron. Soc. **493,** L1 (2020).

[27] G. Cusin, I. Dvorkin, C. Pitrou, and J.-P. Uzan, Phys. Rev. D **100,** 063004 (2019).

[28] S. Wang, V. Vardanyan, and K. Kohri, Phys. Rev. D **106,** 123511 (2022).

[29] S. Mukherjee and J. Silk, Mon. Not. R. Astron. Soc. **491,** 4690 (2020).

[30] S. S. Bavera, G. Franciolini, G. Cusin, A. Riotto, M. Zevin, and T. Fragos, Astron. Astrophys. **660,** A26 (2022).

[31] N. Bellomo, D. Bertacca, A. C. Jenkins, S. Matarrese, A. Raccanelli, T. Regimbau, A. Ricciardone, and M. Sakellariadou, arXiv:2110.15059.

[32] C. Pitrou, G. Cusin, and J.-P. Uzan, Phys. Rev. D **101,** 081301 (2020).

[33] G. Cañas Herrera, O. Contigiani, and V. Vardanyan, Phys. Rev. D **102,** 043513 (2020).

[34] M. Geller, A. Hook, R. Sundrum, and Y. Tsai, Phys. Rev. Lett. **121,** 201303 (2018).

[35] A. C. Jenkins and M. Sakellariadou, Phys. Rev. D **98,** 063509 (2018).

[36] S. Kuroyanagi, K. Takahashi, N. Yonemaru, and H. Kumamoto, Phys. Rev. D **95,** 043531 (2017).

[37] S. Olmez, V. Mandic, and X. Siemens, J. Cosmol. Astropart. Phys. 07 (2012) 009.

[38] E. Dimastrogiovanni, M. Fasiello, A. Malhotra, P. D. Meerburg, and G. Orlando, J. Cosmol. Astropart. Phys. 02 (2022) 040.

[39] L. Valbusa Dall'Armi, A. Mierna, S. Matarrese, and A. Ricciardone, arXiv:2307.11043.

[40] Y. Cui, S. Kumar, R. Sundrum, and Y. Tsai, arXiv: 2307.10360.

[41] P. Adshead, N. Afshordi, E. Dimastrogiovanni, M. Fasiello, E. A. Lim, and G. Tasinato, Phys. Rev. D **103,** 023532 (2021).

[42] E. Dimastrogiovanni, M. Fasiello, and G. Tasinato, Phys. Rev. Lett. **124,** 061302 (2020).

[43] D. Jeong and M. Kamionkowski, Phys. Rev. Lett. **108,** 251301 (2012).

[44] J. Liu, R.-G. Cai, and Z.-K. Guo, Phys. Rev. Lett. **126,** 141303 (2021).

[45] Y. Li, F. P. Huang, X. Wang, and X. Zhang, Phys. Rev. D **105,** 083527 (2022).

[46] V. Domcke, R. Jinno, and H. Rubira, J. Cosmol. Astropart. Phys. 06 (2020) 046.

[47] R. Jinno, T. Konstandin, H. Rubira, and J. van de Vis, J. Cosmol. Astropart. Phys. 12 (2021) 019.

[48] S. Kumar, R. Sundrum, and Y. Tsai, J. High Energy Phys. 11 (2021) 107.

[49] D. Racco and D. Poletti, J. Cosmol. Astropart. Phys. 04 (2023) 054.

[50] L. Bethke, D. G. Figueroa, and A. Rajantie, Phys. Rev. Lett. **111,** 011301 (2013).

[51] L. Bethke, D. G. Figueroa, and A. Rajantie, J. Cosmol. Astropart. Phys. 06 (2014) 047.

[52] L. Valbusa Dall'Armi, A. Nishizawa, A. Ricciardone, and S. Matarrese, Phys. Rev. Lett. **131,** 041401 (2023).

[53] K. N. Ananda, C. Clarkson, and D. Wands, Phys. Rev. D **75,** 123518 (2007).

[54] D. Baumann, P. J. Steinhardt, K. Takahashi, and K. Ichiki, Phys. Rev. D **76,** 084019 (2007).

[55] J. R. Espinosa, D. Racco, and A. Riotto, J. Cosmol. Astropart. Phys. 09 (2018) 012.

[56] K. Kohri and T. Terada, Phys. Rev. D **97,** 123532 (2018).

[57] S. Mollerach, D. Harari, and S. Matarrese, Phys. Rev. D **69,** 063002 (2004).

[58] H. Assadullahi and D. Wands, Phys. Rev. D **81,** 023527 (2010).

[59] G. Domènech, Universe **7,** 398 (2021).

[60] L. Valbusa Dall'Armi, A. Ricciardone, N. Bartolo, D. Bertacca, and S. Matarrese, Phys. Rev. D **103,** 023522 (2021).

[61] P. Auclair et al. (LISA Cosmology Working Group), Living Rev. Relativity **26,** 5 (2023).

[62] C. Ünal, E. D. Kovetz, and S. P. Patil, Phys. Rev. D **103,** 063519 (2021).

[63] A. Malhotra, E. Dimastrogiovanni, M. Fasiello, and M. Shiraishi, J. Cosmol. Astropart. Phys. 03 (2021) 088.

[64] B. Carr, K. Kohri, Y. Sendouda, and J. Yokoyama, Rep. Prog. Phys. **84,** 116902 (2021).

[65] J. M. Maldacena, J. High Energy Phys. 05 (2003) 013.

[66] N. Bartolo, E. Komatsu, S. Matarrese, and A. Riotto, Phys. Rep. **402,** 103 (2004).

[67] T. J. Allen, B. Grinstein, and M. B. Wise, Phys. Lett. B **197,** 66 (1987).

[68] N. Bartolo, S. Matarrese, and A. Riotto, Phys. Rev. D **65,** 103505 (2002).

[69] V. Acquaviva, N. Bartolo, S. Matarrese, and A. Riotto, Nucl. Phys. **B667**, 119 (2003).

[70] F. Bernardeau and J.-P. Uzan, Phys. Rev. D **66**, 103506 (2002).

[71] X. Chen, M.-X. Huang, S. Kachru, and G. Shiu, J. Cosmol. Astropart. Phys. 01 (2007) 002.

[72] X. Chen, Adv. Astron. **2010**, 638979 (2010).

[73] S. Choudhury, A. Karde, K. Dey, S. Panda, and M. Sami, arXiv:2310.11034.

[74] G. Agazie et al. (NANOGrav Collaboration), arXiv:2306.16221.

[75] B. P. Abbott et al. (LIGO Scientific and Virgo Collaborations), Phys. Rev. Lett. **118**, 121102 (2017).

[76] B. P. Abbott et al. (LIGO Scientific and Virgo Collaborations), Phys. Rev. D **100**, 062001 (2019).

[77] R. Abbott et al. (KAGRA, Virgo, and LIGO Scientific Collaborations), Phys. Rev. D **104**, 022005 (2021).

[78] Y.-F. Cai, X. Tong, D.-G. Wang, and S.-F. Yan, Phys. Rev. Lett. **121**, 081306 (2018).

[79] Y.-F. Cai, C. Chen, X. Tong, D.-G. Wang, and S.-F. Yan, Phys. Rev. D **100**, 043518 (2019).

[80] C. Chen and Y.-F. Cai, J. Cosmol. Astropart. Phys. 10 (2019) 068.

[81] C. Chen, X.-H. Ma, and Y.-F. Cai, Phys. Rev. D **102**, 063526 (2020).

[82] D. Langlois and F. Vernizzi, Phys. Rev. D **70**, 063522 (2004).

[83] F. Ferrer, S. Rasanen, and J. Valiviita, J. Cosmol. Astropart. Phys. 10 (2004) 010.

[84] D. Langlois, F. Vernizzi, and D. Wands, J. Cosmol. Astropart. Phys. 12 (2008) 004.

[85] J. Fonseca and D. Wands, J. Cosmol. Astropart. Phys. 06 (2012) 028.

[86] J. Chluba et al., Bull. Am. Astron. Soc. **51**, 184 (2019).

[87] D. Jeong, J. Pradler, J. Chluba, and M. Kamionkowski, Phys. Rev. Lett. **113**, 061301 (2014).

[88] T. Nakama, T. Suyama, and J. Yokoyama, Phys. Rev. Lett. **113**, 061302 (2014).

[89] K. Inomata, M. Kawasaki, and Y. Tada, Phys. Rev. D **94**, 043527 (2016).

[90] R. Allahverdi et al., 10.21105/astro.2006.16182 (2020).

[91] A. D. Gow, C. T. Byrnes, P. S. Cole, and S. Young, J. Cosmol. Astropart. Phys. 02 (2021) 002.

[92] G. Franciolini and A. Urbano, Phys. Rev. D **106**, 123519 (2022).

[93] G. Franciolini, I. Musco, P. Pani, and A. Urbano, Phys. Rev. D **106**, 123526 (2022).

[94] X. Wang, Y.-L. Zhang, R. Kimura, and M. Yamaguchi, Sci. China Phys. Mech. Astron. **66**, 260462 (2023).

[95] M. Sasaki, T. Suyama, T. Tanaka, and S. Yokoyama, Classical Quantum Gravity **35**, 063001 (2018).

[96] B. Carr and F. Kuhnel, Annu. Rev. Nucl. Part. Sci. **70**, 355 (2020).

[97] A. D. Linde and V. F. Mukhanov, Phys. Rev. D **56**, R535 (1997).

[98] D. H. Lyth and D. Wands, Phys. Lett. B **524**, 5 (2002).

[99] K. Enqvist and M. S. Sloth, Nucl. Phys. **B626**, 395 (2002).

[100] D. H. Lyth, C. Ungarelli, and D. Wands, Phys. Rev. D **67**, 023503 (2003).

[101] T. Moroi and T. Takahashi, Phys. Lett. B **522**, 215 (2001); **539**, 303(E) (2002).

[102] N. Bartolo, S. Matarrese, and A. Riotto, Phys. Rev. D **69**, 043503 (2004).

[103] M. Sasaki, J. Valiviita, and D. Wands, Phys. Rev. D **74**, 103003 (2006).

[104] Q.-G. Huang, Phys. Lett. B **669**, 260 (2008).

[105] M. Beltran, Phys. Rev. D **78**, 023530 (2008).

[106] K. Enqvist and S. Nurmi, J. Cosmol. Astropart. Phys. 10 (2005) 013.

[107] K. A. Malik and D. H. Lyth, J. Cosmol. Astropart. Phys. 09 (2006) 008.

[108] S. Pi and M. Sasaki, arXiv:2112.12680.

[109] A. Malhotra, E. Dimastrogiovanni, G. Domènech, M. Fasiello, and G. Tasinato, Phys. Rev. D **107**, 103502 (2023).

[110] E. Silverstein and D. Tong, Phys. Rev. D **70**, 103505 (2004).

[111] M. Alishahiha, E. Silverstein, and D. Tong, Phys. Rev. D **70**, 123505 (2004).

[112] C. Armendariz-Picon, T. Damour, and V. F. Mukhanov, Phys. Lett. B **458**, 209 (1999).

[113] J. Garriga and V. F. Mukhanov, Phys. Lett. B **458**, 219 (1999).

[114] A. Achucarro, J.-O. Gong, S. Hardeman, G. A. Palma, and S. P. Patil, J. Cosmol. Astropart. Phys. 01 (2011) 030.

[115] A. Achúcarro, V. Atal, P. Ortiz, and J. Torrado, Phys. Rev. D **89**, 103006 (2014).

[116] S. Pi, Y.-L. Zhang, Q.-G. Huang, and M. Sasaki, J. Cosmol. Astropart. Phys. 05 (2018) 042.

[117] G. M. Harry (LIGO Scientific Collaboration), Classical Quantum Gravity **27**, 084006 (2010).

[118] F. Acernese et al. (VIRGO Collaboration), Classical Quantum Gravity **32**, 024001 (2015).

[119] K. Somiya (KAGRA Collaboration), Classical Quantum Gravity **29**, 124007 (2012).

[120] S. Hild et al., Classical Quantum Gravity **28**, 094013 (2011).

[121] J. I. Thorpe et al., Bull. Am. Astron. Soc. **51**, 77 (2019).

[122] T. L. Smith, T. L. Smith, R. R. Caldwell, and R. Caldwell, Phys. Rev. D **100**, 104055 (2019); **105**, 029902(E) (2022).

[123] W.-R. Hu and Y.-L. Wu, Natl. Sci. Rev. **4**, 685 (2017).

[124] C. L. Carilli and S. Rawlings, New Astron. Rev. **48**, 979 (2004).

[125] N. Seto, S. Kawamura, and T. Nakamura, Phys. Rev. Lett. **87**, 221103 (2001).

[126] S. Kawamura et al., Prog. Theor. Exp. Phys. **2021**, 05A105 (2021).

[127] V. F. Mukhanov, Sov. Phys. JETP **67**, 1297 (1988).

[128] M. Sasaki, Prog. Theor. Phys. **76**, 1036 (1986).

[129] M. Sasaki and E. D. Stewart, Prog. Theor. Phys. **95**, 71 (1996).

[130] A. A. Starobinsky, JETP Lett. **42**, 152 (1985).

[131] D. Wands, K. A. Malik, D. H. Lyth, and A. R. Liddle, Phys. Rev. D **62**, 043527 (2000).

[132] D. H. Lyth, K. A. Malik, and M. Sasaki, J. Cosmol. Astropart. Phys. 05 (2005) 004.

[133] K. Kohri, C.-M. Lin, and T. Matsuda, Phys. Rev. D **87**, 103527 (2013).

[134] Y. Tada and S. Yokoyama, Phys. Rev. D **91**, 123534 (2015).

[135] E. Komatsu and D. N. Spergel, Phys. Rev. D **63**, 063002 (2001).

[136] Y. Akrami *et al.* (Planck Collaboration), Astron. Astrophys. **641**, A9 (2020).

[137] M. Maggiore, Phys. Rep. **331**, 283 (2000).

[138] P. Adshead, K. D. Lozanov, and Z. J. Weiner, J. Cosmol. Astropart. Phys. 10 (2021) 080.

[139] H. V. Ragavendra, Phys. Rev. D **105**, 063533 (2022).

[140] K. T. Abe, R. Inui, Y. Tada, and S. Yokoyama, J. Cosmol. Astropart. Phys. 05 (2023) 044.

[141] R.-G. Cai, S. Pi, and M. Sasaki, arXiv:1810.11000.

[142] C. Unal, Phys. Rev. D **99**, 041301 (2019).

[143] V. Atal and G. Domènech, J. Cosmol. Astropart. Phys. 06 (2021) 001.

[144] H. V. Ragavendra, P. Saha, L. Sriramkumar, and J. Silk, Phys. Rev. D **103**, 083510 (2021).

[145] C. Yuan and Q.-G. Huang, Phys. Lett. B **821**, 136606 (2021).

[146] C. Yuan, D.-S. Meng, and Q.-G. Huang, arXiv:2308.07155.

[147] S. Garcia-Saenz, L. Pinol, S. Renaux-Petel, and D. Werth, J. Cosmol. Astropart. Phys. 03 (2023) 057.

[148] F. Zhang, Phys. Rev. D **105**, 063539 (2022).

[149] G. Domènech and M. Sasaki, Phys. Rev. D **97**, 023521 (2018).

[150] J. Garcia-Bellido, M. Peloso, and C. Unal, J. Cosmol. Astropart. Phys. 09 (2017) 013.

[151] T. Nakama, J. Silk, and M. Kamionkowski, Phys. Rev. D **95**, 043511 (2017).

[152] S. Wang, T. Terada, and K. Kohri, Phys. Rev. D **99**, 103531 (2019); **101**, 069901(E) (2020).

[153] M. Braglia and S. Kuroyanagi, Phys. Rev. D **104**, 123547 (2021).

[154] R. K. Sachs and A. M. Wolfe, Astrophys. J. **147**, 73 (1967).

[155] G. Capurri, A. Lapi, L. Boco, and C. Baccigalupi, Astrophys. J. **943**, 72 (2023).

[156] C. T. Byrnes, E. J. Copeland, and A. M. Green, Phys. Rev. D **86**, 043512 (2012).

[157] D.-S. Meng, C. Yuan, and Q.-G. Huang, Phys. Rev. D **106**, 063508 (2022).

[158] K. Saikawa and S. Shirai, J. Cosmol. Astropart. Phys. 05 (2018) 035.

[159] A. M. Green, A. R. Liddle, K. A. Malik, and M. Sasaki, Phys. Rev. D **70**, 041502 (2004).

[160] R.-G. Cai, Z.-K. Guo, J. Liu, L. Liu, and X.-Y. Yang, J. Cosmol. Astropart. Phys. 06 (2020) 013.

[161] Z. Zhou, J. Jiang, Y.-F. Cai, M. Sasaki, and S. Pi, Phys. Rev. D **102**, 103527 (2020).

[162] Y.-F. Cai, J. Jiang, M. Sasaki, V. Vardanyan, and Z. Zhou, Phys. Rev. Lett. **127**, 251301 (2021).

[163] Z.-Z. Peng, C. Fu, J. Liu, Z.-K. Guo, and R.-G. Cai, J. Cosmol. Astropart. Phys. 10 (2021) 050.

[164] R.-G. Cai, C. Chen, and C. Fu, Phys. Rev. D **104**, 083537 (2021).

[165] K. Inomata, M. Braglia, X. Chen, and S. Renaux-Petel, J. Cosmol. Astropart. Phys. 04 (2023) 011; 09 (2023) E01.

[166] D.-S. Meng, C. Yuan, and Q.-G. Huang, Sci. China Phys. Mech. Astron. **66**, 280411 (2023).